

Methods and Procedures for Predicting Cable Roll-off in Sensor Measurements

Part I:

Full Bridge Measurements

Alan R. Szary
Thomas P. Gerber
Douglas R. Firth

Precision Filters, Inc.

Ithaca, New York
(607) 277-3550
E-mail: sales@pfinc.com



PRECISION FILTERS, INC.

Transducer Conditioning Systems ■ Filter/Amplifier Systems ■ Signal Switching Systems

1. Introduction

The bandwidth of a measurement system that includes a bridge-based sensor, such as a strain gage, piezo-resistive accelerometer, or pressure sensor, is affected by the capacitance of the connecting cable interacting with the sensor output impedance. Termed cable roll-off, this frequency response – typically characterized in terms of the -3 dB cutoff frequency of an equivalent RC filter – can be calculated, but requires knowledge of the sensor resistance, cable resistance, and cable capacitance. These values can be difficult to measure and are not always specified by cable manufacturers.

In this paper, we formulate cable roll-off relations for a measurement system comprised of a full-bridge differential circuit. We explain how to obtain the applicable cable capacitance of paired (often called twisted-pair) and non-paired multi-conductor shielded cables using manufacturer specifications or, when required, benchtop measurements. We also show how the applicable resistance can be determined from specified values for the bridge sensor output resistance and cable series resistance. Roll-off predictions are then presented for measurement circuits connected by two standard cable types (paired and non-paired, respectively) and compared to roll-off measurements obtained using a benchtop method. We conclude by demonstrating how Precision Filters' AC shunt calibration can be used to directly measure cable roll-off in situ and provide end-to-end bandwidth verification for an entire measurement system.

2. Problem Scope and Bounds

Most technical literature on the analysis of cables and their characteristics is focused on the transmission of high speed digital data or RF communications. In these applications, specifications for a cable's characteristic impedance, line loss, and reflection coefficients are critical. Yet such properties are less important at the relatively low frequencies encountered in the environment of mechanical test and measurement (DC to 100s of kHz).

The system of interest in the present study is depicted in Figure 1. Here a full Wheatstone bridge with gages in 1, 2, or 4 arms is connected via a shielded cable to a signal conditioner input; any necessary completion resistors are collocated with the sensor. The signal conditioner provides sensor excitation, common-mode noise rejection (via the differential input), amplification, and filtering. The inherent sensor bandwidth, as specified by the manufacturer, can be hundreds of kHz. Proper attention must be paid to the cable capacitance and resistance or severe limitations to the overall frequency response of the measurement system will result.

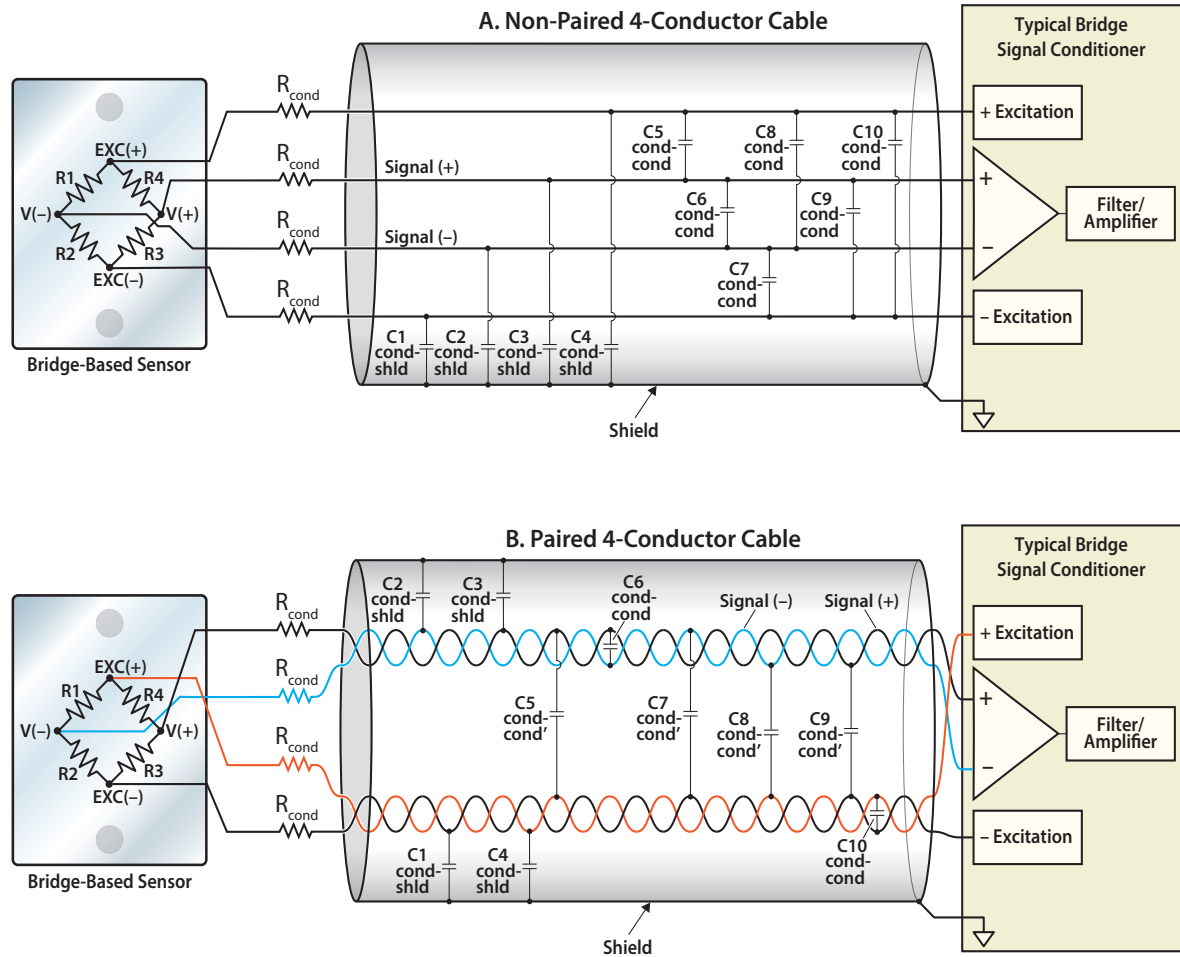


Figure 1. Diagrams depicting the measurement system and cables of interest in this study. (A) Non-paired 4-conductor cable connected to a full-bridge sensor on one end and an analog signal conditioner on the other. (B) Paired (and twisted) 4-conductor cable in the same arrangement. Note that, as shown, the (+) and (-) excitation lines are connected to one wire pair and the (+) and (-) signal lines to the other wire pair.

To address the effects of cabling in mechanical test and measurement applications, we proceed by making the following assumptions:

- A paired or non-paired 4-conductor cable connects on the sensor end to a strain gage or Wheatstone bridge with an output impedance ranging from 100 Ω to roughly 10 k Ω depending on the sensor used.
- The unspooled cable connects on the other end to a signal conditioner with high input impedance on the order of 100 k Ω to 100 M Ω .
- Frequencies of interest are sufficiently low to allow for an accurate lumped-parameter analysis of the cable. This criterion is easily met for frequencies up to a few hundred kHz on cables a few hundred feet in length.
- Cable shields are used for electrostatic shielding and are normally tied to ground at only one side of the cable.

We also recognize that in multi-conductor cables such as those depicted in Figure 1, multiple capacitances exist between the cable conductors and shield (indexed C1-C10 in Figure 1). In the analysis that follows, we invoke the following definitions:

- A capacitance exists from each conductor to the cable shield, referred to here as $C_{cond-shld}$. We assume all conductor-to-shield capacitances ($C_{cond-shld}$) are equal.
- In a non-paired multi-conductor cable, a capacitance exists from each conductor to any other conductor, referred to here as $C_{cond-cond}$. We assume all conductor-to-conductor capacitances ($C_{cond-cond}$) are equal.
- In a paired multi-conductor cable, two conductor-to-conductor capacitances exist. The within-pair capacitance, measured between the conductors in each pair, is denoted $C_{cond-cond}$. The between-pair capacitance, measured between any two conductors in different pairs, is denoted $C'_{cond-cond}$. We further assume that all within-pair capacitances are equal and all between-pair capacitances are equal, but $C_{cond-cond} \neq C'_{cond-cond}$.

3. Model Formulation

To describe the cable roll-off of a bridge-based sensor working into a cable under the conditions stated above, we model the sensor and cable as a single-pole low-pass RC filter (Figure 2). The roll-off of such a filter is characterized by a transfer function $H(f)$ with an amplitude response defined by

$$|H| = \frac{1}{\sqrt{1 + (2\pi RCf)^2}} \quad (1)$$

where R is a lumped resistance (Ω), C is a lumped capacitance (F), and f is frequency (Hz). The roll-off defined by (1) can be normalized in terms of the cutoff frequency f_c ,

$$f_c = \frac{1}{2\pi RC} \quad (2)$$

Between (1) and (2), notice that the amplitude attenuation is 3 dB ($= 1/\sqrt{2}$) at the cutoff frequency. Hence f_c defines a reference frequency that delineates the roll-off from passband to stopband (Figure 2), and provides a useful metric for comparing the relative bandwidth of different cables.

Use of the preceding relations to predict the frequency response of the measurement circuit in Figure 1 requires estimation of the appropriate capacitance and resistance. In the following sections, we show how to reduce the circuit to a form amenable to analysis by (1), where R and C are defined in terms of measurable quantities.



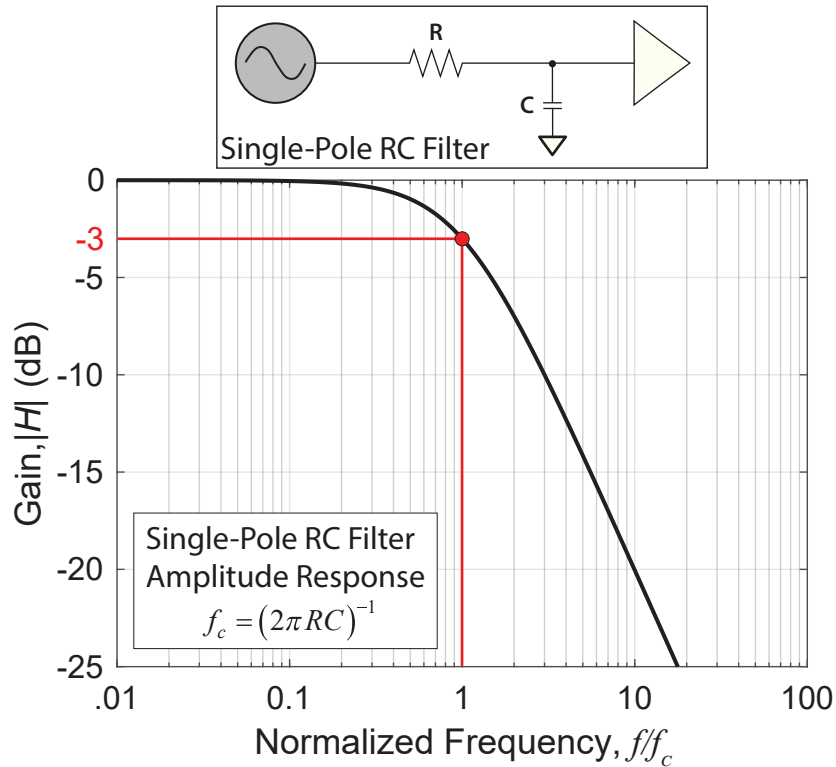


Figure 2. Diagram (top) and normalized frequency response (bottom) of a single-pole RC filter. The attenuation is 3 dB at the cutoff frequency f_c .

3.1 The Total Capacitance

The capacitance C in (1) and (2) is a function of the conductor-to-conductor ($C_{cond-cond}$, $C'_{cond-cond}$) and conductor-to-shield ($C_{cond-shld}$) capacitances, with a form that depends on the wiring of the measurement circuit. Refer again to Figure 1A. To proceed, it is important to recognize that the cable shield is grounded to provide electrostatic shielding, so we can treat it as circuit ground in our analysis. Furthermore, because the (+) and (–) excitation supplies are highly regulated, the impedance to ground for the excitation lines is low and can be treated as circuit ground. Consequently, capacitances C_1 , C_4 , and C_{10} can be neglected, and our analysis of the circuit can be reduced to the diagram shown in Figure 3, where the excitation lines and shield are referenced as ground. It should now be apparent that the parallel capacitance to ground from each of the signal lines ($C_2, 7, 8$ on $V(-)$; $C_3, 5, 9$ on $V(+)$) equates to $C_{cond-shld} + 2C_{cond-cond}$, as shown in Figure 4.

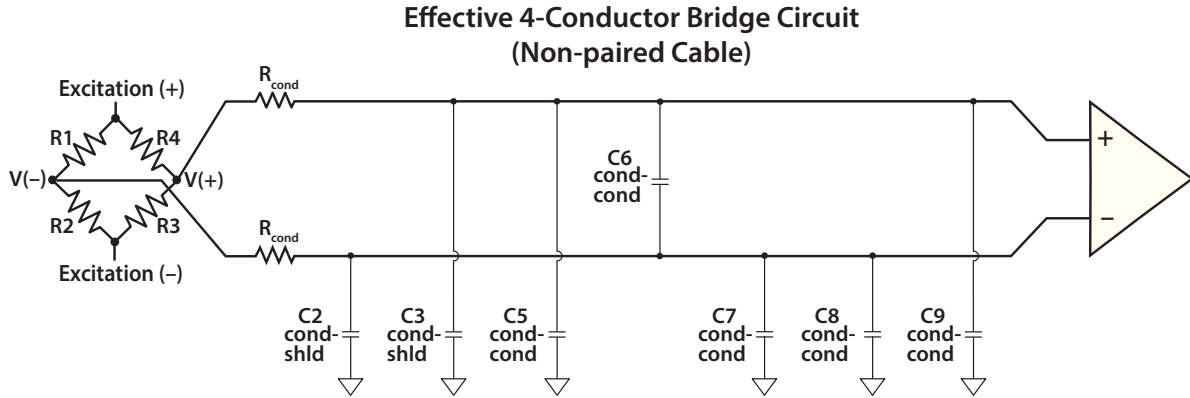


Figure 3. Effective full-bridge circuit used in the analysis of total capacitance on the signal lines (compare with Figure 1A).

The remaining capacitance (C_6) is between the signal lines. In a full bridge, this capacitance can be decomposed into two equal capacitances to ground, denoted C_{6A} and C_{6B} in Figure 4, that are in series. Since two equal capacitances in series sum to half the component capacitances, C_{6A} and C_{6B} must each have a capacitance equal to $2C_{cond-cond}$. Adding C_{6A} to the $V(+)$ signal line and C_{6B} to the $V(-)$ signal line gives the total capacitance on each signal output as

$$C_{total} = C_{cond-shld} + 4C_{cond-cond} \quad (3)$$

Note that because the bridge is balanced and symmetric, we can analyze the roll-off on only one of the signal lines – with C equal to C_{total} as defined in (3) – since the roll-off on the opposite line will be equivalent.

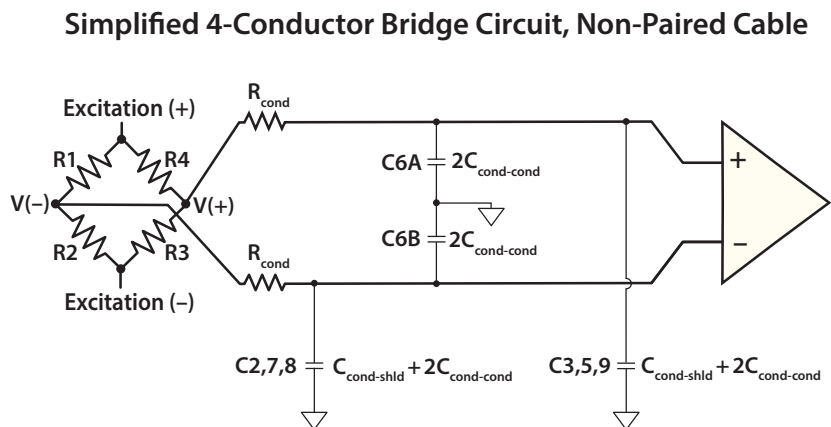


Figure 4. Summary of circuit model used to derive the total capacitance C_{total} on each of the signal lines for a non-paired 4-conductor cable. The total capacitance defined by (3) applies to both the $V(+)$ and $V(-)$ signal lines.



Figure 5 shows the same simplified 4-wire bridge circuit for a paired cable. The result is the same except for C_6 : because the capacitance between the signal lines is a within-pair capacitance (i.e. $C'_{cond-cond} \neq C_{cond-cond}$), we must retain an extra term in (3) for the paired cable:

$$C_{total} = C_{cond-shld} + 2C_{cond-cond} + 2C'_{cond-cond} \quad (4)$$

Simplified 4-Conductor Bridge Circuit, Paired Cable

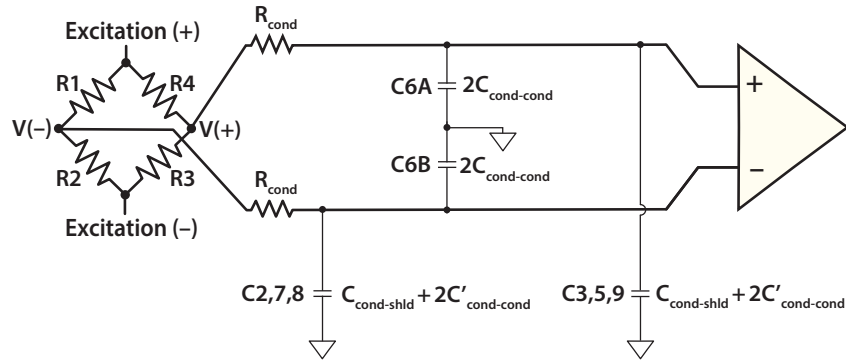


Figure 5. Summary of circuit model used to derive the total capacitance C_{total} on each of the signal lines for a paired 4-conductor cable. The total capacitance defined by (4) applies to both the V(+) and V(-) signal lines.

3.2 The Total Resistance

The resistance R in (1) and (2) includes both the sensor output resistance and the cable series resistance. As noted in Section 3.1, the balanced symmetry of the full bridge circuit translates to equivalent total capacitances (defined by (3) and (4)) on each of the signal lines (V(+) and V(-) in Figure 3-Figure 5). This symmetry applies to the signal output resistance as well, so we need only consider the output resistance on one of the signal lines (V(+) in Figure 6). This resistance is a parallel combination of the R3 and R4 bridge arm resistances, conventionally denoted as the Thevenin resistance $R3//R4$. In many modern bridge-based sensors (e.g. MEMS accelerometers and pressure sensors), this output resistance can vary significantly from sensor to sensor due to variations in the microfabrication process. Fortunately, most sensor calibration sheets report an output resistance R_{out} that represents the specified measured resistance between the bridge corners when the excitation lines are floating. This output resistance is related to the Thevenin bridge output resistance as

$$R3//R4 \approx \frac{R_{out}}{2} \quad (5)$$

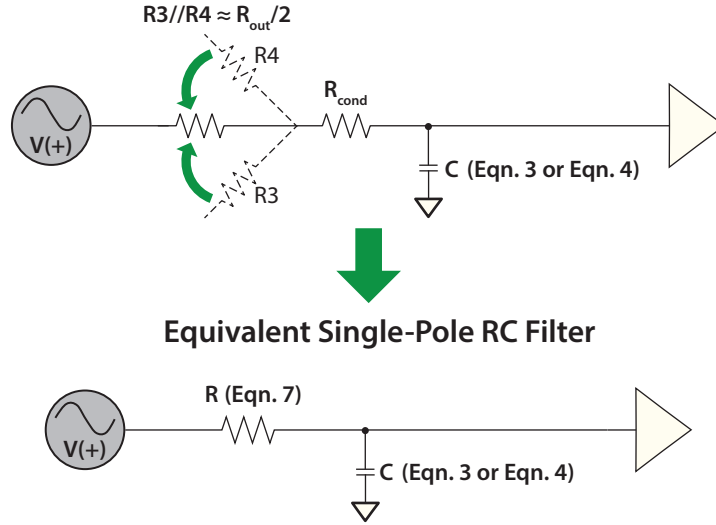


Figure 6. (Top) Depiction of the Thevenin sensor output resistance $R3//R4$ and cable series resistance R_{cond} that act on the total cable capacitance. **(Bottom)** Summary model of sensor-cable combination as a single-pole RC filter (compare with Figure 2). C is defined by Equation (3) for a non-paired cable and by Equation (4) for a paired cable; R is defined by Equation (7).

The total resistance also includes a contribution from the series resistance of the cable conductors. In measurement circuits with low-impedance sensors and long runs of small-diameter, high-resistance wire, this series resistance cannot be ignored. The series resistance is distributed over the entire length of the conductor, and is commonly specified by manufacturers as a DC resistance R_{cond} (commonly reported per unit length in Ω/ft). In the Appendix (A.1), we show that the apparent resistance of the conductor R_a , defined as the real part of its complex impedance Z , scales with the DC resistance as

$$R_a = \frac{R_{cond}}{3} \quad (6)$$

It is this apparent resistance, and not the full series resistance of the conductor, that must be added to the sensor output resistance to obtain an accurate estimate of the total resistance (Figure 6):

$$R_{total} = \frac{R_{out}}{2} + \frac{R_{cond}}{3} \quad (7)$$

Note that since we are determining the roll-off on only one of the signal lines ($V(+)$; Figure 6), R_{cond} is the DC resistance over the length of cable between the sensor and the signal conditioner.

3.3 Model Summary

Our model of the cable as a single-pole RC filter is summarized in Figure 6. Equating C_{total} defined in (3) and (4) to C in (2) and substituting R_{total} defined



by (7) for R , we can express the cutoff frequencies, f_c , for non-paired and paired cables as, respectively,

$$f_c = \left(2\pi \left(\frac{R_{out}}{2} + \frac{R_{cond}}{3} \right) (C_{cond-shld} + 4C_{cond-cond}) \right)^{-1} \quad (8)$$

$$f_c = \left(2\pi \left(\frac{R_{out}}{2} + \frac{R_{cond}}{3} \right) (C_{cond-shld} + 2C_{cond-cond} + 2C'_{cond-cond}) \right)^{-1} \quad (9)$$

This model applies to a full-bridge differential circuit with any number of active arms connected to a signal conditioner by a multi-conductor cable, so long as the completion resistors are collocated with the active arms. In the following section, we demonstrate how to use (8) and (9) to predict cable roll-off in a measurement system with a bridge-based MEMS accelerometer and two industry-standard, 4-conductor shielded cables. We also show how to verify those predictions by using a benchtop setup to obtain direct roll-off measurements.

4. Test Application

To evaluate the performance of our model on a real measurement system, we consider two sensor-cable combinations (Table 1). One of the cables is non-paired (PCB Piezotronics Inc., Model 034) and one is paired (Belden Inc., Model 82502); each is combined with the same MEMS accelerometer (PCB 3501). The specifications listed in Table 1 are taken directly from manufacturer specification sheets [Ref. 1-2] and/or calibration sheets [Ref. 3].

Table 1. Cable and Sensor Specifications					
Cables				Sensor	
Model	Type (# of Conductors)	Conductor-to-Conductor Capacitance, C_{scc} (pF/ft)	Conductor DC Resistance, R_{cond} (Ω /ft)	Model	Specified Output Resistance, R_{out} (Ω)
PCB 034	Non-paired (4)	14	Unspecified	PCB 3501*	6544**
Belden 82502	Paired (4)	25	0.024	PCB 3501*	6544**
*PCB 3501B1220KG MEMS accelerometer (SN#11009)					
**From calibration sheet [Ref. 3]					

In most cases, the required resistances R_{cond} and R_{out} are clearly specified. If not (e.g. R_{cond} for the PCB 034), the specified values can be obtained directly from the manufacturer or, if necessary, directly measured using standard benchtop instruments. Relating specified cable capacitances to the total capacitance C_{total} defined by (3) and (4) is, however, less straightforward.



Standard cable capacitance specifications [Ref. 1-2, 4] include what is conventionally termed a *conductor-to-conductor* capacitance, as given in Table 1. (Cable specifications commonly include other capacitances, but they are not relevant to the analysis presented here.) Importantly, this manufacturer-specified *conductor-to-conductor* capacitance – which we denote C_{scc} – does not equate to $C_{cond-cond}$ as defined in Section 2 and Figure 1. The benchtop setup for measuring C_{scc} on a non-paired cable is shown in Figure 7, where we make use of the same notation introduced in Section 2.

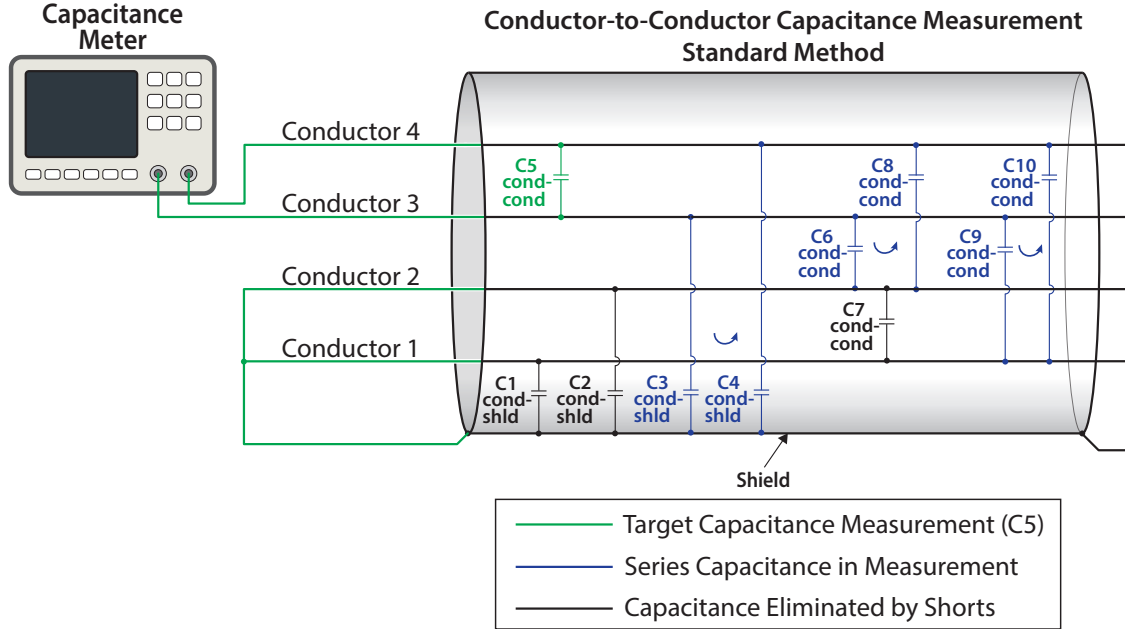


Figure 7. Standard method for measurement of the *conductor-to-conductor* capacitance specification (here denoted as C_{scc}) on a non-paired cable. The notation used for the component capacitances is consistent with PFI's conventions (compare with Figure 1A).

In the arrangement shown, a capacitance is measured between conductors 3 and 4 with the remaining conductors and shield tied together. The target capacitance is therefore C_5 ($C_{cond-cond}$). However, the configuration will include capacitance from three additional parallel paths: C_3 ($C_{cond-shld}$) in series with C_4 ($C_{cond-shld}$), C_6 ($C_{cond-cond}$) in series with C_8 ($C_{cond-cond}$), and C_9 ($C_{cond-cond}$) in series with C_{10} ($C_{cond-cond}$). Taking these series combinations into account, we can express the actual measured capacitance, C_{scc} , in terms of $C_{cond-cond}$ and $C_{cond-shld}$ ¹:

$$C_{scc} = \frac{C_{cond-shld}}{2} + 2C_{cond-cond} \quad (10)$$

The measurement defined by (10) should yield a value for C_{scc} – the manufacturer-specified *conductor-to-conductor* capacitance – of 14 pF/ft for the non-paired

¹ For the case of n -conductors in the same measurement setup, the relation generalizes to:

$$C_{scc} = \frac{1}{2}(C_{cond-shld} + nC_{cond-cond})$$



PCB 034 cable (Table 1). Comparing (10) to (8), it should be readily apparent that the cutoff frequency of the non-paired PCB 034 cable can be expressed as

$$f_c = \left(4\pi \left(\frac{R_{out}}{2} + \frac{R_{cond}}{3} \right) C_{scc} \right)^{-1} \quad (11)$$

This relation can be used to predict the roll-off on a non-paired 4-conductor cable with DC resistance R_{cond} , sensor output resistance R_{out} , and a manufacturer-specified capacitance C_{scc} that represents the measurement shown in Figure 7. Note that R_{cond} and C_{scc} are conventionally specified per unit length and must therefore be multiplied by the length of the cable run between the sensor and the signal conditioner (see Appendix A.1).

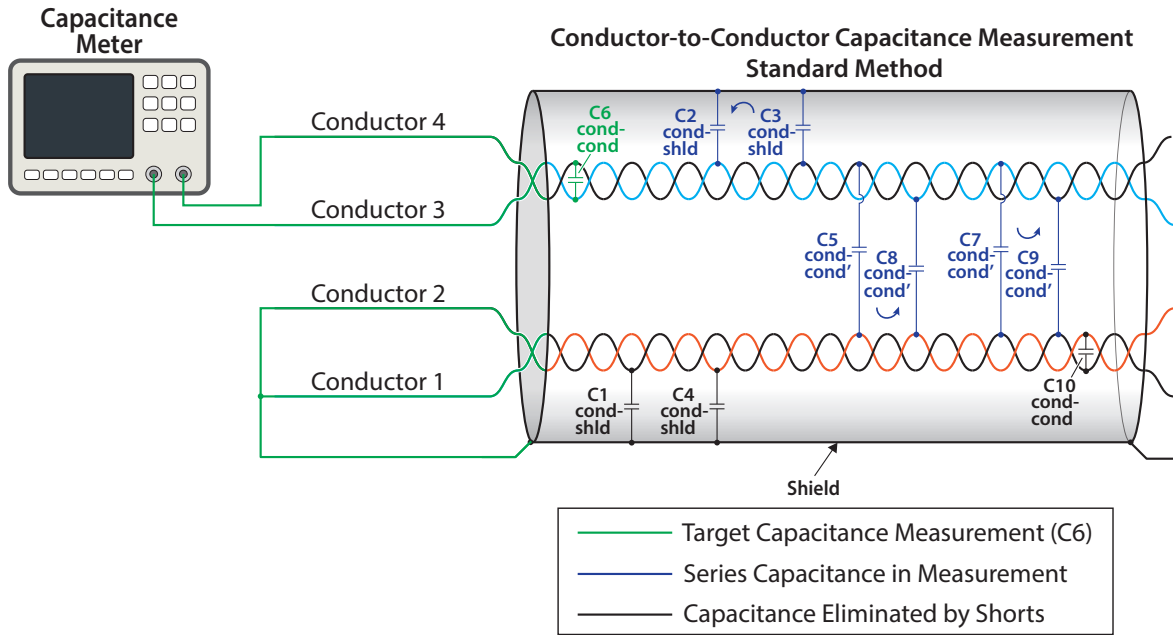


Figure 8. Standard method for measurement of the *conductor-to-conductor* capacitance specification (here denoted as C_{scc}) on paired cables. The notation used for the component capacitances is consistent with PFI's conventions (compare with Figure 1B).

The corresponding measurement setup for the manufacturer-specified *conductor-to-conductor* capacitance C_{scc} of a paired cable is shown in Figure 8. Again, the target capacitance (C6) is not the only capacitance in the measurement: three other series combinations must also be accounted for, so the relation in (10) extends to the paired cable as²:

$$C_{scc} = \frac{C_{cond-shld}}{2} + C_{cond-cond} + C'_{cond-cond} \quad (12)$$

Comparing (12) and (9), it should be clear that the cutoff frequency defined by (11) applies to both non-paired and paired cables with manufacturer-specified

² For the case of m -conductor pairs in the same measurement setup, the relation generalizes to:

$$C_{scc} = \frac{C_{cond-shld}}{2} + C_{cond-cond} + (m-1)C'_{cond-cond}$$

conductor-to-conductor capacitances (C_{scc}) defined by (10) and (12), respectively.

To summarize, our model for each cable in a full-bridge measurement circuit (i.e. Figure 1 and Equation 11) with a specific PCB 3501 MEMS sensor (6544 Ω output impedance) is given in Table 2. A cable length of 150 ft is selected as a reasonable stand-off distance that might be employed in hazardous field testing. As our aim in this paper is to demonstrate an expedient method for roll-off estimation, we use the manufacturer-specified *conductor-to-conductor* capacitances (C_{scc}) to generate the predictions that follow. It should be emphasized, however, that these capacitances are nominal values and are typically provided as a reference rather than a rigorous value. Moreover, when considering other cable models, care should be taken to ensure that specified *conductor-to-conductor* capacitances are consistent with Figure 7 and Figure 8 (i.e. equate to C_{scc}) before using (11) to make roll-off predictions.

Table 2. Model Summary*					
Cable				Sensor	
Model	Length (ft)	R_{cond} (Ω/ft)	C_{scc} (pF/ft)	Model	R_{out} (Ω)
PCB 034	150	.293**	14 [†]	PCB 3501	6544 [†]
Belden 82502	150	.024 [†]	25 [†]	PCB 3501	6544 [†]
*Equation (11)					
**Measured for this study					
[†] Manufacturer-specified (see Table 1)					
[‡] Manufacturer-specified <i>conductor-to-conductor</i> capacitance (see Table 1)					

The capacitance C_{scc} can be verified using the same benchtop setup depicted in Figure 7 and Figure 8 or, alternatively, by determining the component capacitances $C_{cond-shld}$, $C_{cond-cond}$, and $C'_{cond-cond}$ using a series of properly designed measurements. In a companion paper [Ref. 3], direct measurements of C_{scc} for the PCB 034 and Belden 82502 are reported³ as 14.05 pF/ft and 22.95 pF/ft, respectively. Despite the discrepancy for the Belden cable, the difference translates to predicted cutoff frequencies that vary by less than 10%.

In the following section, we introduce a benchtop method for acquiring direct roll-off measurements using a real cable and a simulated version of a specific sensor.

4.1 Benchtop Roll-off Measurement

Roll-off measurements on each of the cables listed in Table 1 and Table 2 were performed using the procedure illustrated in Figure 9. Resistors were selected at the driven end of the cable to simulate the output resistance of the PCB 3501 MEMS accelerometer.

³ They report measured values for C_{total} as defined in (3) and (4), where $C_{total} = 2C_{scc}$.

For this setup to accurately represent a realistic sensor-cable field configuration, the following requirements must be met:

- The entire length of cable (here 150 ft) is unspooled.
- The cable shield is grounded to ensure equivalence with run-time conditions.
- The (+) and (–) excitation lines are connected to ground at the signal conditioner side of the cable to simulate the same low impedance output of the constant voltage excitation supply.
- A differential signal is applied to the (+) signal and (–) signal wires through a differential attenuator made up of discrete resistors equal to R_{out} and $2R_{out}$, where R_{out} is the output resistance of the selected sensor (here the PCB 3501; see Table 1 and Table 2).
- If the signal generator has non-zero output impedance (typically $50\ \Omega$, as shown in Figure 9), this resistance should be subtracted from the upper bridge-simulating resistor for improved accuracy of the roll-off measurement.

With these requirements satisfied, the frequency response of the simulated measurement circuit was determined by sweeping the signal generator from 100 Hz to 100 kHz.

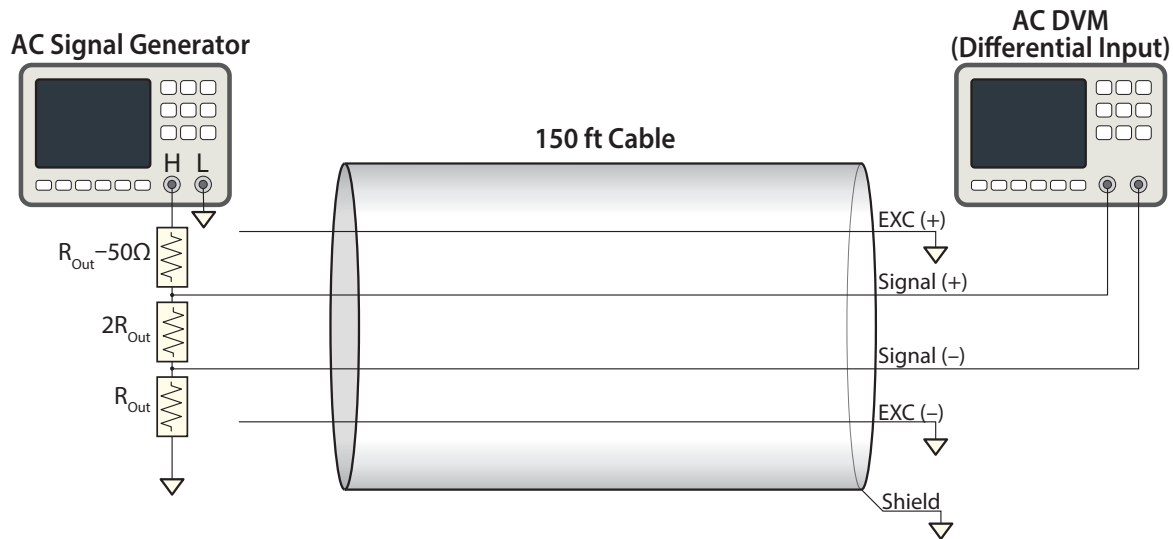


Figure 9. Benchtop setup used to measure cable roll-off on the sensor-cable combinations in Table 2.

4.2 Results and Implications

The modeled and measured frequency responses of each sensor-cable combination are shown in Figure 10. The satisfactory agreement between modeled and measured roll-off gives us confidence in the first-order (RC) representation of the cable transfer function. The measured cutoff frequencies for both cables are in excellent agreement ($< 10\%$ error) with the predicted values.

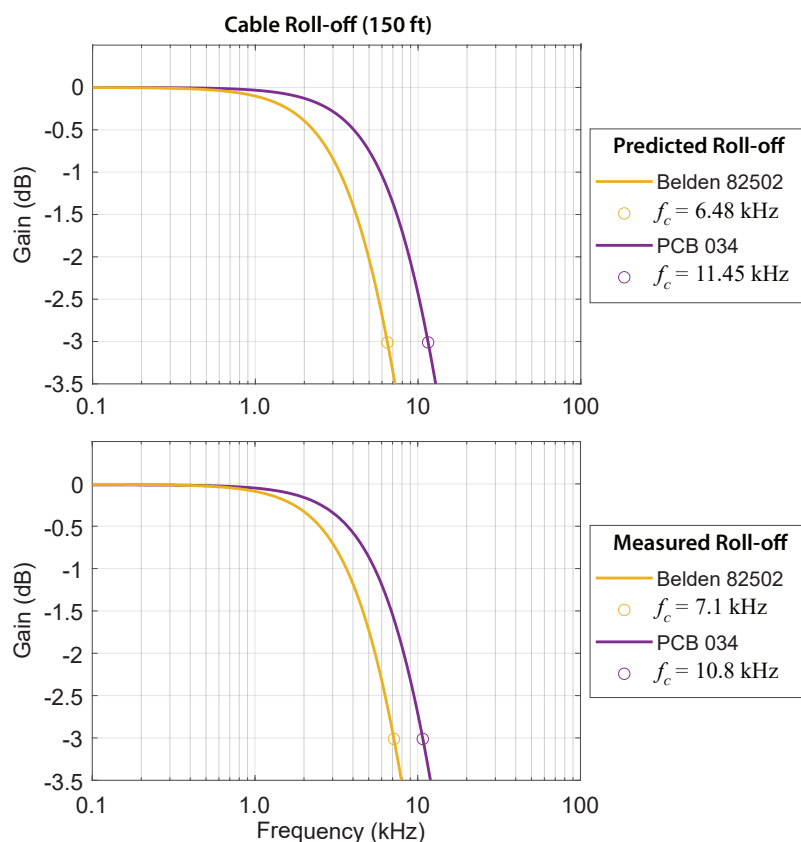


Figure 10. Modeled (**top**) and measured (**bottom**) frequency response of the cable-sensor pairs summarized in Table 2. The modeled response was calculated using (1) and (11) with the parameters listed in Table 2. The measured response was obtained using the setup described in Section 4.1. The -3 dB cutoff frequencies (f_c) are also plotted and given in the legends.

The results presented in Figure 10 highlight the implications of our analysis for measurement system design and test planning. Regardless of the bandwidth capabilities of the signal conditioning equipment employed, the sensor-cable combination can be the limiting factor that determines the effective measurement bandwidth. To see this more clearly, in Figure 11 and Figure 12 we construct design charts for the Belden 82502 and PCB 034 cables based on a standard requirement for signal preservation of no more than 5% attenuation (.45 dB). The charts show how this requirement combines with the sensor output resistance and cable length

to limit the effective bandwidth of the sensor-cable combination. For example, if a 10 kHz bandwidth is required for a measurement system that includes a Belden 82502 cable in a full-bridge connection to a sensor with an output resistance of $3000\ \Omega$, the cable length must be kept below 70 ft to ensure signal preservation ($\leq 5\%$ attenuation) over the required bandwidth. If the PCB 034 cable were used, the maximum cable length would be 125 ft. It is important to realize that, though often overlooked, cable roll-off can determine whether a measurement system will meet a specified bandwidth requirement.

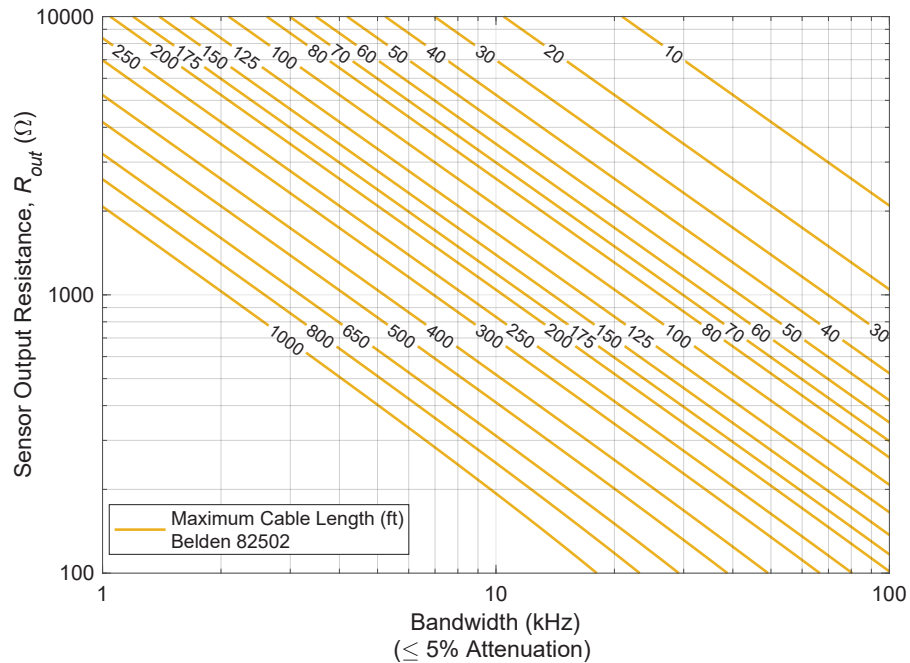


Figure 11. Design chart illustrating the cable length limitations on the effective bandwidth for the Belden 82502 based on the model summarized in Table 2. Here, the effective bandwidth is defined as the spectral range over which the amplitude attenuation is less than 5%. Given a required bandwidth and a sensor with a specified output resistance R_{out} , the plot can be used to determine the maximum permissible length of Belden 82502 cable in a full-bridge measurement circuit.

Notice that over most of the parameter space covered in Figure 11 and Figure 12, we observe – for a given cable length, capacitance, and series resistance – the scaling $B \sim 1/R_{out}$, where B is the bandwidth corresponding to the maximum allowable attenuation. This is a consequence of the sensor output resistance R_{out} dominating the comparatively small series resistance in (11). Deviations from this scaling only occur for long runs of higher-resistance PCB 034 cable connected to a sensor with low output resistance (Figure 12).

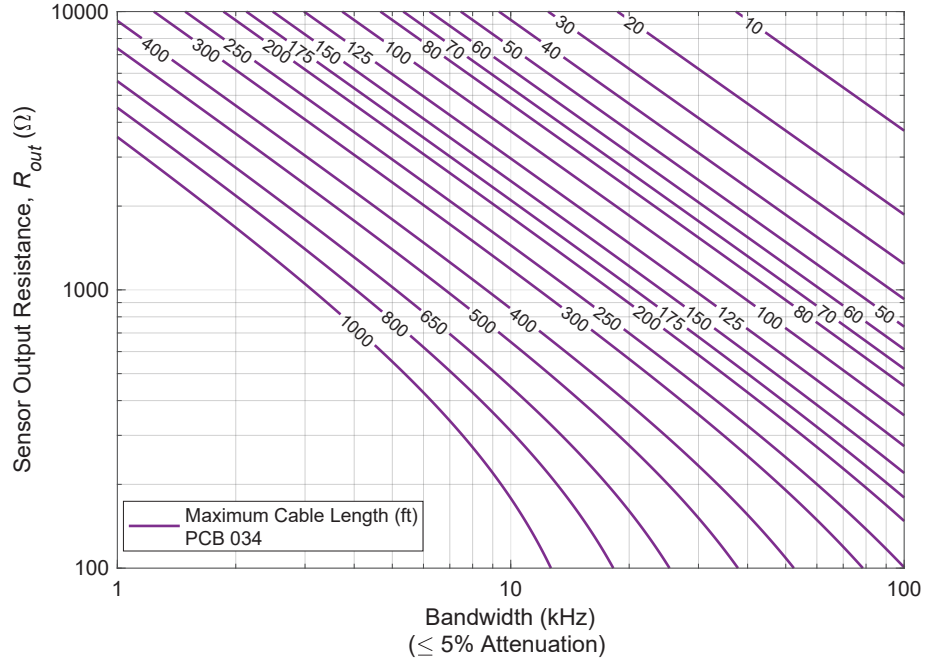


Figure 12. Design chart illustrating the cable length limitations on the effective bandwidth for the PCB 034 based on the model summarized in Table 2. Here, the effective bandwidth is defined as the spectral range over which the amplitude attenuation is less than 5%. Given a required bandwidth and a sensor with a specified output resistance R_{out} , the plot can be used to determine the maximum permissible length of PCB 034 cable in a full-bridge measurement circuit.

We can formulate relations between the cutoff frequency defined by (11) and the effective measurement bandwidth for any level of attenuation. If the measurement requirement is stated as a maximum % attenuation, A_{pct} , the corresponding bandwidth B is

$$B = f_c \sqrt{10^4 \left(100 - A_{pct}\right)^{-2} - 1} \quad (13)$$

If the measurement requirement is stated as a maximum attenuation A_{dB} in dB down (i.e. $A_{dB} \geq 0$), the corresponding bandwidth B is

$$B = f_c \sqrt{10^{0.1 A_{dB}} - 1} \quad (14)$$

In the Appendix (A.2), we provide explicit expressions for generating design charts like those shown in Figure 11 and Figure 12 for any properly specified cable and sensor, along with a relation that can be used to directly calculate the maximum cable length given a bandwidth requirement and a maximum allowable attenuation.



5. Measuring Roll-off In situ: AC Shunt Calibration

The methodology introduced in this paper can be readily applied to the design of a new measurement system to ensure the bandwidth requirements are met. We recognize, however, that our approach may not be practical for some existing installations. In a complicated test layout, cable disassembly for benchtop measurements is problematic (if feasible), and may involve multiple types and lengths of legacy cable with unknown or unverifiable specifications. Field-based installations present additional challenges, as it is often difficult and time-consuming to obtain sensitive measurements using specialized equipment in variable conditions. For cases like these, an expedient in situ method to obtain reliable pre-test roll-off predictions is required.

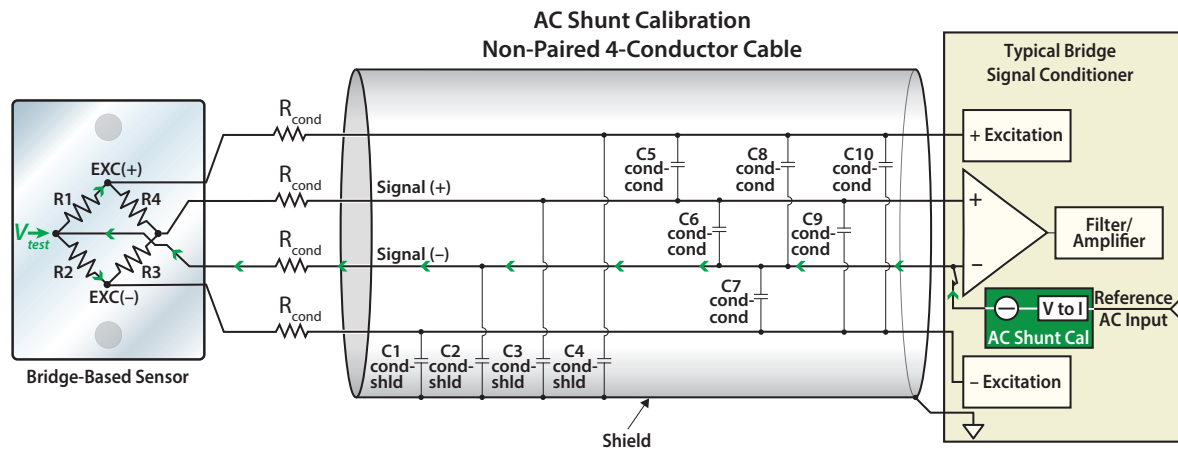


Figure 13. Diagram illustrating AC shunt calibration in the measurement system from Figure 1A. The AC shunt calibration circuitry is a built-in feature of the analog signal conditioner [Ref. 5].

To address this need, Precision Filters has developed a proprietary technology called AC Shunt Calibration [Ref. 5] which enables the direct measurement of cable roll-off from the convenience of the instrumentation room. In AC shunt calibration, an AC current is injected into the R1/R2 bridge corner (Figure 13). This current interacts with the actual output resistance of the bridge corner to produce a sensor-based test signal V_{test} that is equal to $I \cdot R_{out}/2$. As the frequency of the test signal is increased, the interaction of the cable with the sensor's output resistance produces a very similar frequency response to that produced by the MEMS element within the active sensor. The roll-off can then be determined by comparing the test signal to the measured bridge output.

To demonstrate the efficacy of AC shunt calibration for roll-off verification, in Figure 14 we compare the predicted response of the Belden 82502 reported earlier – 150ft of unspooled cable connected to the same PCB 3501 accelerometer – with

the measured shunt calibration response of the same sensor-cable combination connected to a Precision Filters signal conditioner. The modeled and measured roll-off show satisfactory agreement.

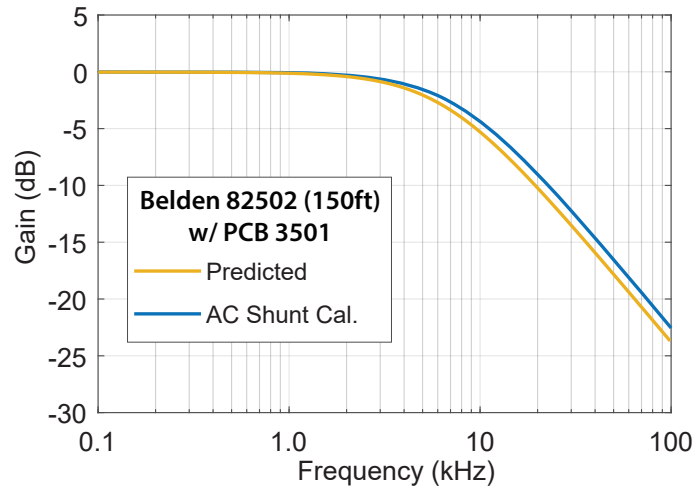


Figure 14. Predicted roll-off of the Belden 82502 cable connected to a PCB 3501 accelerometer (see Table 2) compared with the measured roll-off obtained using AC shunt calibration on the same sensor-cable combination. Note that the roll-off plot is extended beyond the cutoff frequency (compare with Figure 10).

6. Summary

Cable roll-off is an important and yet often overlooked consideration in the design of high-performance measurement systems. Our aim in this paper is to raise awareness of cable roll-off among measurement engineers and test planners and provide a systematic approach to characterizing it. As shown here, a multi-conductor cable connected to a bridge-based sensor can be modeled as a single-pole RC filter with a first-order frequency response. The apparent simplicity of this approach belies the challenge of obtaining accurate estimates of R and C : their formulation varies with the design of the measurement circuit, and they depend on parameters that may not be directly specified by cable manufacturers. By demonstrating methods to obtain sufficiently accurate estimates of R and C for the purpose of modeling roll-off, along with a benchtop procedure for measuring roll-off on real cables, we hope to enable a more rigorous assessment of cable response in cases where it can significantly limit the bandwidth of a measurement system. For a practical application of the methods described in this paper, readers are referred to a companion publication [Ref. 3] that addresses the bandwidth-limiting effects of cable roll-off on shock measurements.



7. Acknowledgments

We thank Dr. Patrick Walter for helpful comments that greatly improved this paper, and Kyle Brown for assisting with the laboratory measurements used in our study.

8. References Cited

- [1] PCB Piezotronics Specification Sheet 31858: Lightweight Shielded Four Conductor Cable, Model 034. Revision D (5/11/2009), ECN #30657.
- [2] Belden Product Specification Sheet: 82502 2-Pair Cable. Revision Number 0.285 (3/16/2021).
- [3] Walter, P.L., Szary, A., and Woernley, J. 2021. MEMS Shock Accelerometer Signal Modification Attributable to the Electrical Impedance of Their Cables. PCB Piezotronics White Paper, 33pp.
- [4] ASTM Designation D4566-20 (2020). Standard Test Methods for Electrical Performance Properties of Insulations and Jackets for Telecommunications Wire and Cable. ASTM International, DOI: 10.1520/D4566-20, 54pp.
- [5] Precision Filters Product Specification Sheet, P8465 (Rev. G): Precision 28124 Quad-Channel Transducer Conditioner with Voltage and Current Excitation, 12pp.

A. Appendix

A.1 Conductor Model

As depicted in Figure 15, the conductor is modeled as a chain of unit-length sections, each consisting of a resistive and capacitive element. All sections have the same DC resistance per unit length \hat{R}_{cond} and capacitance per unit length \hat{C} .

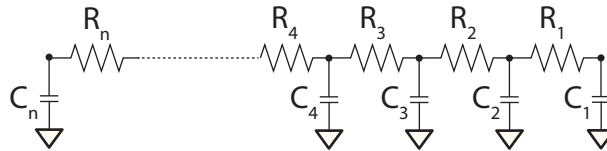


Figure 15. Model of a conductor as a chain of RC elements.

The impedance Z_1 of the first section is

$$Z_1 = Z_R + Z_C = \hat{R}_{cond} + (j\omega\hat{C})^{-1} \quad (\text{A.1})$$

where ω is angular frequency. Proceeding down the conductor, adding the resist-

ance of section $(n+1)$ in series and its capacitance in parallel, we have

$$Z_{n+1} = \frac{Z_n Z_C}{Z_n + Z_C} + Z_R \quad (\text{A.2})$$

where

$$Z_R = \hat{R}_{cond} \quad (\text{A.3})$$

$$Z_C = (j\omega\hat{C})^{-1} = -jb_c, \quad b_c = (\omega\hat{C})^{-1} \quad (\text{A.4})$$

Expanding the complex impedances in (A.2) and making use of (A.3) and (A.4), we can write

$$Z_n = a_n - jb_n \quad (\text{A.5})$$

and

$$Z_{n+1} = \hat{R}_{cond} + \frac{a_n b_c^2}{(a_n^2 + (b_n + b_c)^2)} - j \frac{b_c b_n^2 + b_n b_c^2 + a_n^2 b_c}{(a_n^2 + (b_n + b_c)^2)} \quad (\text{A.6})$$

Equation (A.6) defines a first-order recursion equation for the real (a_n) and imaginary (b_n) components of the complex impedance Z_n with an initial condition specified by (A.1). To make progress, we recognize that cable capacitance is typically on the order of 10^{-11} F/ft. For a nominal frequency of 10 kHz, the impedance b_c is on the order of 10^5 - 10^6 Ω /ft. Given typical resistive impedance of 10^{-2} - 10^{-1} Ω /ft, we can approximate

$$a_n \ll b_c \quad (\text{A.7})$$

With (A.7), the real and imaginary parts of (A.6) reduce to

$$a_{n+1} \approx \hat{R}_{cond} + \frac{a_n b_c^2}{(b_n + b_c)^2} \quad (\text{A.8})$$

$$b_{n+1} \approx \frac{b_c b_n^2 + b_n b_c^2}{(b_n + b_c)^2} = \frac{b_c b_n}{b_c + b_n} \quad (\text{A.9})$$

The recursion relation in (A.9) is now uncoupled from (A.8); its solution, for an initial condition $b_1 = b_c$, is

$$b_n = \frac{b_c}{n} \quad (\text{A.10})$$

Substituting relation (A.10) into (A.8) and simplifying, we have



$$a_{n+1} = \hat{R}_{cond} + \left(\frac{n^2}{(1+n)^2} \right) a_n \quad (\text{A.11})$$

If we now define a uniform section length δx such that $x = n\delta x$, where x is the distance along the cable, and substitute this relation into (A.11) we have, after simplifying,

$$a(x + \delta x) = \hat{R}_{cond} \delta x + \left(\frac{x^2}{(x + \delta x)^2} \right) a(x) \quad (\text{A.12})$$

Subtracting $a(x)$ from both sides and dividing by δx gives

$$\frac{a(x + \delta x) - a(x)}{\delta x} = \hat{R}_{cond} + \frac{1}{\delta x} \left(\frac{x^2}{(x + \delta x)^2} - 1 \right) a(x) \quad (\text{A.13})$$

The LHS of (A.13) is the spatial derivative of $a(x)$, the apparent resistance, in finite difference form, i.e.

$$\frac{da}{dx} = \lim_{\delta x \rightarrow 0} \frac{a(x + \delta x) - a(x)}{\delta x} \quad (\text{A.14})$$

By rewriting the second term on the RHS of (A.13) as

$$\left(\frac{x^2 - (x + \delta x)(x + \delta x)}{\delta x (x + \delta x)(x + \delta x)} \right) a(x) = \left(\frac{-2x - \delta x}{(x + \delta x)(x + \delta x)} \right) a(x) \quad (\text{A.15})$$

the limit in (A.14) is found to be

$$\frac{da}{dx} = -2ax^{-1} + \hat{R}_{cond} \quad (\text{A.16})$$

A solution to (A.16), given the boundary condition $a(x=0) = 0$, is

$$a(x) = \frac{\hat{R}_{cond}}{3} x \quad (\text{A.17})$$

Comparing (A.17) to the DC resistance of the cable (i.e. $R_{cond}(x) = \hat{R}_{cond}x$), we see that the apparent resistance a , denoted R_a in (6), increases linearly with cable length at 1/3 the rate of the DC resistance.

Combining (A.17) with the continuous form of (A.10) and substituting from (A.4), we can express the impedance of the conductor as a function of the cable length x :

$$Z(x) = \frac{\hat{R}_{cond}}{3} x - j \frac{1}{\omega \hat{C} x} \quad (\text{A.18})$$

Adding the sensor output resistance from (5) in series with the cable, we have

$$Z(x) = \frac{R_{out}}{2} + \frac{\hat{R}_{cond}}{3} x - j \frac{1}{\omega \hat{C} x} \quad (\text{A.19})$$

The impedance in (A.19) is that of a low-pass RC filter circuit. The corresponding transfer function can be expressed in standard form as

$$H(j\omega) = \frac{V_{out}(j\omega)}{V_{in}(j\omega)} = \frac{(j\omega C)^{-1}}{R + (j\omega C)^{-1}} = \frac{1}{1 + j\omega RC} \quad (\text{A.20})$$

where

$$R = \frac{R_{out}}{2} + \frac{\hat{R}_{cond}}{3} x, \quad C = \hat{C}x, \quad \omega = 2\pi f \quad (\text{A.21})$$

The magnitude of (A.20), with R and C defined by (A.21), defines the amplitude response of the cable-sensor pair:

$$|H| = \frac{1}{\sqrt{1 + (\omega RC)^2}} \quad (\text{A.22})$$

Equation (A.22) is equivalent to Equation (1) with $\omega = 2\pi f$. Note that C represents the total capacitance as explained in Section 3.1.

A.2 Cable Roll-off Relations

The design charts in Figure 11 and Figure 12 can be generated for any properly specified sensor-cable combination in a 4-wire, full-bridge configuration. Referring back to (1), we can define the fractional level of attenuation as

$$A = 1 - |H| \quad (\text{A.23})$$

Substituting this relation into (1) and setting $f = B$, where B is the bandwidth over which the attenuation is less than or equal to A , we have

$$B = \alpha (2\pi RC)^{-1} = \alpha f_c \quad (\text{A.24})$$

$$\alpha = \sqrt{(1 - A)^{-2} - 1} \quad (\text{A.25})$$

As noted above, cable capacitance and resistance specifications are typically reported per unit length. Denoting \hat{R}_{cond} as the specified series resistance per unit length (as in Appendix A.1), \hat{C}_{scc} as the manufacturer-specified *conductor-to-conductor* capacitance per unit length, and L as the cable length, we can recast (A.24) using (11):

$$B = \alpha \left(4\pi \hat{C}_{scc} L \left(\frac{R_{out}}{2} + \frac{\hat{R}_{cond}}{3} L \right) \right)^{-1} \quad (\text{A.26})$$

Equation (A.26) can be used to generate design charts such as those shown in Figure 11 and Figure 12. We can also solve (A.26) for L , permitting direct calculation of the maximum allowable cable length when the required bandwidth and maximum allowable attenuation are specified:



$$L = \frac{3\alpha}{\beta R_{out} + \sqrt{\beta(4\alpha \bar{R}_{cond} + \beta R_{out}^2)}} \quad (\text{A.27})$$

$$\beta = 3\pi B \hat{C}_{sc} \quad (\text{A.28})$$

Note that for (A.27) and (A.28) to be valid for the preferred units of length (e.g. ft or m), resistance must be given in Ω , capacitance in F, and bandwidth in Hz.

Precision Filters, Inc.

Ithaca, New York

(607) 277-3550

E-mail: sales@pfinc.com



PRECISION FILTERS, INC.

Transducer Conditioning Systems ■ Filter/Amplifier Systems ■ Signal Switching Systems

Copyright © 2021 by Precision Filters, Inc.